Microfluidics Lab

Srishti Krishnan (1010908813)

Introduction

Microfluidics is a multidisciplinary field that involves the comprehensive study and manipulation of fluids on the micro (10^{-9}) scale. The applications of microfluidics research and innovations extend to molecular and evolutionary biology, optics and photonics, and cellular biology and cancer treatment.

The purpose of this experiment is to analyse the behaviour of fluid flow through a microfluidics chip. The chip consists of 4 channels and 5 distinct regions - the straight section, the sudden convergence, the gradual convergence, the square bend and the v-bend ([1] figure 2). The observation of the flow is done via a microscope, and images of the different magnified fields are taken by the *LAS* imaging software.

The objective of the lab is to better understand two governing equations - Bernoulli's equation and the Hagen-Poiseuelle equation.

Bernoulli's equation: $P + \frac{1}{2}\rho v^2 + \rho g z = constant$ (1)

Hagen-Poiseuelle equation: $Q = \frac{s^2}{8\pi\mu L}(\Delta p + \rho g \Delta z)$ (2)

Experimental Procedure

The driving source of the microfluidic flow is a syringe containing working fluid, which is connected to the chip inlet. The syringe is suspended from a retort stand at a variable height, so that the fluid flows due to the effect of gravity. The outlet of the chip is connected to a waste reservoir tube, which collects the working fluid after it passes through the chip.

The height of the syringe relative to the chip can be varied to change the velocity of the microfluidic flow, since by Bernoulli's equation, velocity and height difference related by $v = \sqrt{2gz}$.

The device used to measure the flow velocity was a microscope connected to the *LAS* software. The microscope was set to 10x magnification, and adjustment of the positioning and resolution of the field of view was done through the focus knob and stage adjustment rods. The images taken on the software were adjusted via the exposure, gain and saturation settings. Streaks are measured easiest as pixel lengths. To convert the pixel length of the streaks in each image to a physical length, the 100 micrometer scale on the image was measured as 159μm, giving a conversion factor of 1px = 0.629μm. The conversion factor was multiplied by each streak to find its physical length.

Errors and Error Analysis (1 page)

I. Quantifiable Errors

The main quantifiable errors are those in distance, height, time, and consequently velocity.

The distance uncertainty is taken to be ±1 pixel, which by the scale factor gives ±0.629μm. Reading uncertainty in height from the ruler is ±0.5mm. The time uncertainty is taken to be 0.5ms, as listed on the software [2] used to measure lengths of streaks. The formula for error propagation for velocity is

$$\Delta v = v \cdot \sqrt{(\frac{\Delta x}{x})^2 + (\frac{\Delta t}{t})^2}$$

Distance (x) [μm]	Uncertainty in distance (Δx) [μm]	Time, i.e. Exposure (t) [ms]	Uncertainty in time (Δt) [ms]	Velocity (v) [μm/s]	Uncertainty in velocity (Δv) [μm/s]
4.669	0.629	134.1	0.500	348.181	46.918

Figure 1: One row of raw data collected to determine the velocity profile in the straight channel. This data is plotted in figure 2 with uncertainties in velocity shown as horizontal error bars.

The roughness of the wall is the other quantifiable imperfection in the straight channel. This is quantified by measuring the distance of ten points away from the ideal wall location. The standard deviation of this points is calculated using the formula

$$s = \sqrt{\frac{\Sigma(x - \bar{x})^2}{n-1}}$$

The standard deviation was calculated to be 1.561μm±0.629μm relative to a channel width of 950μm. Thus, the relative roughness of the channel is 0.164%, which is insignificant relative to other sources of uncertainty. The roughness of the wall introduces marginal friction, which may decrease the velocity of the fluid due to frictional energy loss. Compared to an ideal smooth decrease in pressure, significant roughness can cause flow irregularities like eddies and recirculations that cause a non-linear pressure-drop downstream, but is unlikely to occur here.

II. Non-quantifiable errors

There are certain non-quantifiable errors and assumptions made in this experiment. The main assumption is that the chip manufacturer makes the height of the chip uniform throughout, so height remains constant, and only with changes. Other assumptions include potential debris and imperfection within the channels. The non-quantifiable errors in this experiment are bubbles and debris that disrupt microfluidic flow.

Results and Discussion

Straight Channels

The flow of the fluid in the straight channels is laminar, as indicated by smooth pathlines and a lack of turbulent mixing.

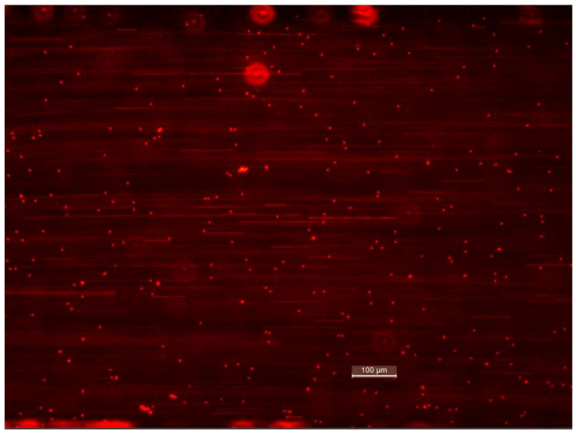

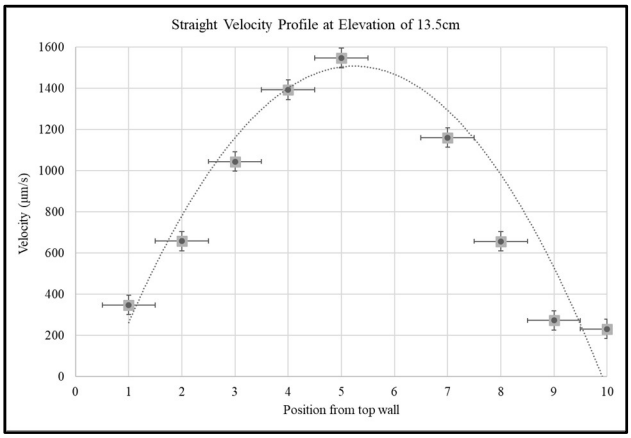

(a) (b)

Figure 2 (a) the LAS image captured of the straight channel (b). Velocity profile for the straight channel at a syringe height of 13.5cm. The points are fit to a 2nd degree polynomial best fit curve, with error bars as depicted in figure 1.

The velocity profile from 2(b) shows a parabolic curve that is rightward convex, with the largest velocity at the center decreasing quadratically to the edges. This is similar to the velocity profile for laminar flow in a circular pipe.

From the Hagen- Poiseuille equation (2), maximum velocity must occur at the center (r=0), and minimum velocity must occur at the walls (r = width of the channel), due to the no-slip condition along the walls of the straight channel. Experimental data matches this prediction.

There is an increasing gradient for rate of increase of velocity from the walls to the center of the straight channel. The velocity value at both extremes are not exactly 0, since the magnification of 10x prevented us from capturing an image of the entire channel. The top and bottom bounds of the image are taken to be the top and bottom walls of the straight channel instead.

The mean velocity of the straight channel can be manipulated by varying certain parameters of the Bernoulli equation. This is done by changing the height of the syringe, changing the density of the working fluid, and changing the pressure by expelling liquid using the syringe plunger.

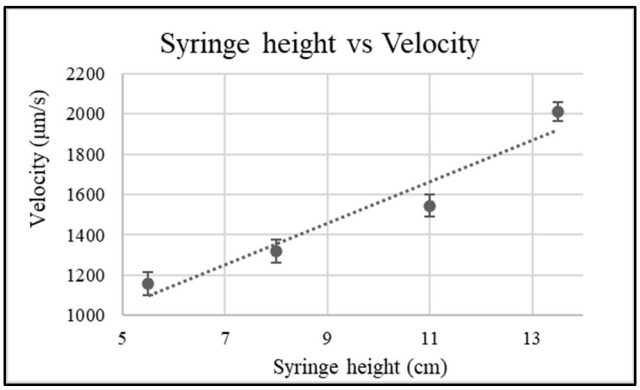

Figure 3. Syringe height against velocity at 4 different heights. Points are fit to a linear best-fit line. Horizontal uncertainties are too small to be seen. Vertical uncertainties from figure 1

To determine the relationship between z_1 and V_3, firstly, the relationship between Q and del(p) is derived for each section. These expressions are combined to get an expression for P_1-P_6. This gives

$$P_1 - P_6 = Q8\pi\mu L\left(\frac{1}{(s_1)^2} + \frac{3}{(s_2\ )^2} + \frac{1}{(s_3)^2}\right) - \rho g(z_1 - z_3)$$

P_1 and P_2 are equal, giving

$$\frac{Q8\pi\mu L}{\rho g}\left(\frac{1}{(s_1)^2} + \frac{3}{(s_2\ )^2} + \frac{1}{(s_3)^2}\right) = (z_1 - z_3)$$

Since $Q=U_3S_3$, giving the relationship between U_3 and z_1, that is

$$U_3S_3\frac{8\pi\mu L}{\rho g}\left(\frac{1}{(s_1)^2} + \frac{3}{(s_2\ )^2} + \frac{1}{(s_3)^2}\right) = (z_1 - z_3),$$

Ie, $U_3S_3 \propto (z_1 - z_3)$, showing a linear relationship.

Channels of Different Size

I. Comparing theoretical and experimental centerline flow velocity ratio

For sudden convergence, using the scaling factor of 100μm= 159px, the initial width is 944.099μm±0.629μm (1501px), and the final width is 337.267μm±0.629μm (536px). Assuming height along the chip is unchanged and the working fluid is incompressible, the incompressible continuity equation

$$A_1v_1 = A_2v_2\ (3)$$

is used, giving a final-to-initial velocity ratio of **2.80**. For gradual convergence, the initial width is 622.604μm±0.629μm and the final width is 338.598μm±0.629μm. The incompressible continuity equation gives a velocity ratio of **1.84**.

Experimentally, the sudden convergence channel causes an increase in velocity from 243.968μm/s to 634.317μm/s, giving a velocity ratio of **2.60**, with a percentage error of 7.80% compared to the theoretical value. The experimental value is larger because v_2 is smaller than it was predicted to be, due to the friction caused by wall roughness, and turbulent energy loss. Additionally, measurement uncertainties also contribute to the discrepancy.

The gradual convergence channel causes an increase in velocity from 563.729μm/s to 975.872μm/s, giving a velocity ratio of **1.73**. This experimental value has a percentage error of 6.30% compared to the theoretical value. Once again, the experimental value is larger due to frictional losses. However, the percentage error is much smaller than that for the sudden convergence. This may be due to the ease of measuring pathlines due to lesser turbulence.

II. Exploring pathlines as an indicator of turbulent flow

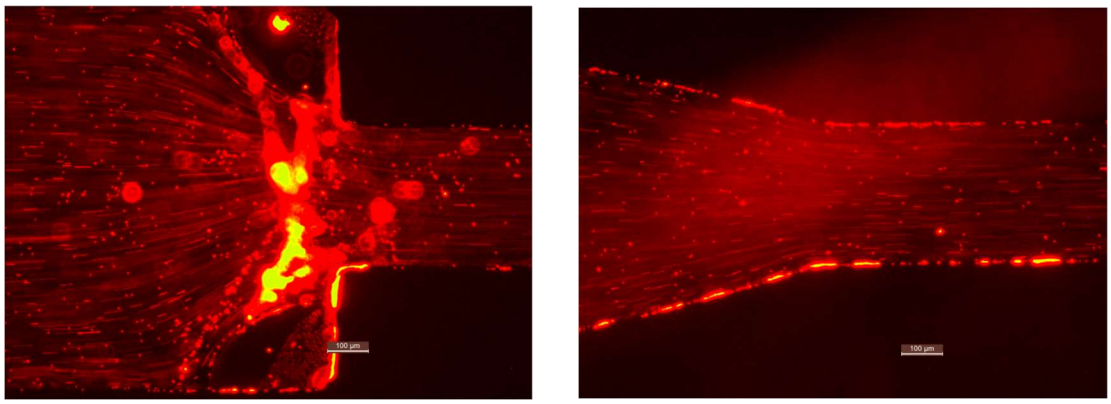

(a) (b)

Figure 3: (a) the sharp convergence and (b) the gradual convergence.

The fast movement of the particles created pathlines that indicate the movement of fluid flow. These pathlines vary with channel geometries. Both the sudden and gradual convergences had straight pathlines initially.

The abrupt transition in the sudden convergence channel caused pathlines to curve dramatically towards the neck of the channel, becoming straight after the convergence. However, the presence of eddies is not noticed in our images. The gradual convergence, in the absence of the abrupt transition, had mostly straight pathlines, with curves only at the neck of the convergence. The pathlines remain straight along and near the centerline of flow.

In our images, turbulent flow is not observed. Pathlines are straight and do not intersect with each other. However, there are large air bubbles near the neck of the sudden convergence channel which interrupt the flow, and hence, it cannot be determined whether the sudden convergence would ideally introduce turbulence.

Flow transitions, that is, transitions between laminar and turbulent flow, are ubiquitous because it is common for laminar flow to turn turbulent when the narrow region of ideal conditions that support laminar flow (having a Reynold's number below the critical value) are disturbed. This can happen in piping systems, HVAC systems, etc. Smoother transitions decrease the friction that the flow experiences against the walls of the container, which decreases the frictional energy loss. Velocity loss is thus decreased, so that the speed of the flow is not altered greatly.

Channels with Bends - The Square Bend and the V-Bend

The fluid in both channels is laminar before and after the bend, and pathlines change according to channel geometry. Significant circulation or turbulence is not visible in the images captured, since non-continuous motion or fluctuations that indicate these phenomena are not noticed.

In the concave corner of the stream tube, inertial forces push the fluid against the walls, widening the tube. Conversely, the fluid flow in the convex corners of the stream tube are relatively slower, creating a low-velocity region that causes compression of the tube. Fast moving fluid avoids the convex corner, and creates a boundary layer that rounds the corner sharply.

Due to the continuity equation (3), the velocities must remain unchanged before and after the bend. However, experimental values show discrepancies. For the v-bend, the initial velocity of 553.697±52.137μm is 1.24 times larger than the final velocity of 448.181±46.260μm. For the square bend, the initial velocity of 691.053μm is 2.75 times larger than the final velocity of 251.713μm. These discrepancies could be due to frictional energy losses, the directional change, and the effect of air bubbles in the crevices on the channels disrupting fluid flow. Systematic errors, such difficulty measuring velocity exactly at the centerline, also add to the differences.

Conclusions

The aims of this experiment were to analyse the behaviour of fluid in the 4 channels of the microfluidic chip using the Bernoulli and Hagen-Poiseuelle equations. The Bernoulli dependence of velocity and height was verified, and the Hagen-Poiseuelle theory of parabolic velocity profile was confirmed. This analysis demonstrated the significant effects that friction, through wall roughness, channel imperfections and bubbles, can have on the behaviour of fluids – further solidifying the importance of engineering solutions in mitigating frictional energy losses. Most results differed from theory by insignificant amounts, attributed to the aforementioned frictional losses, and hence can be reproduced. However, those results which varied from theoretical expectation significantly, such as those for channels with bends, are not reproducible, and vary

primarily due to experimental error. Improvements to the experimental method include averaging streaklengths over several measurements to reduce the effect of anomalies.

Bibliography

[1] AER210 Microfluidics Lab Manual (accessed Nov. 19, 2025)

[2] “Microfluidic Flow Annotator,” Microfluidic Flow Annotator - Beta, https://hayson.me/My_Website/microfluidicthing/ (accessed Nov. 13, 2025).